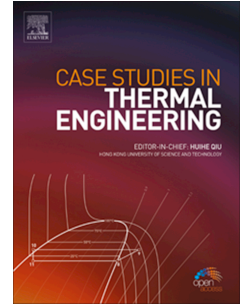


# Journal Pre-proof

Flow characteristics and heat transfer performance in a Y-Fractal mini/microchannel heat sink

Lixiao Liang, Jibiao Hou, Xiangjun Fang, Ying Han, Jie Song, Le Wang, Zhanfeng Deng, Guizhi Xu, Hongwei Wu



PII: S2214-157X(19)30335-1

DOI: <https://doi.org/10.1016/j.csite.2019.100522>

Reference: CSITE 100522

To appear in: *Case Studies in Thermal Engineering*

Received Date: 8 August 2019

Revised Date: 26 August 2019

Accepted Date: 26 August 2019

Please cite this article as: L. Liang, J. Hou, X. Fang, Y. Han, J. Song, L. Wang, Z. Deng, G. Xu, H. Wu, Flow characteristics and heat transfer performance in a Y-Fractal mini/microchannel heat sink, *Case Studies in Thermal Engineering* (2019), doi: <https://doi.org/10.1016/j.csite.2019.100522>.

This is a PDF file of an article that has undergone enhancements after acceptance, such as the addition of a cover page and metadata, and formatting for readability, but it is not yet the definitive version of record. This version will undergo additional copyediting, typesetting and review before it is published in its final form, but we are providing this version to give early visibility of the article. Please note that, during the production process, errors may be discovered which could affect the content, and all legal disclaimers that apply to the journal pertain.

© 2019 Published by Elsevier Ltd.

# Flow Characteristics and Heat Transfer Performance in a Y-Fractal Mini/Microchannel Heat Sink

Lixiao Liang<sup>1</sup>, Jibiao Hou<sup>1</sup>, Xiangjun Fang<sup>2\*</sup>, Ying Han<sup>2</sup>, Jie Song<sup>1</sup>, Le Wang<sup>1</sup>,  
Zhanfeng Deng<sup>1</sup>, Guizhi Xu<sup>1</sup>, Hongwei Wu<sup>3\*</sup>

<sup>1</sup>State Key Laboratory of Advanced Power Transmission Technology (Global Energy Interconnection Research Institute, Changping District, Beijing, 102211, China)

<sup>2</sup>School of Energy and Power Engineering, Beihang University, Beijing, 100191, China

<sup>3</sup>School of Engineering and Computer Science, University of Hertfordshire, Hatfield, AL10 9AB, UK

\*Corresponding author: Prof. Xiangjun Fang, Email: [07761@buaa.edu.cn](mailto:07761@buaa.edu.cn)

Dr. Hongwei Wu, Email: [h.wu6@herts.ac.uk](mailto:h.wu6@herts.ac.uk)

## Abstract:

This article presents a combined experimental and computational study to investigate the flow and heat transfer in a Y-fractal microchannel. Experimental apparatus was newly built to investigate the effect of three different control factors, i.e., fluid flow rate, inlet temperature and heat flux, on the heat transfer characteristics of the microchannel. A standard k- $\epsilon$  turbulence computational fluid dynamics (CFD) model was developed, validated and further employed to simulate the flow and heat transfer microchannel. A comparison between simulated results and the obtained experimental data was presented and discussed. Results showed that good agreement was achieved between the current simulated results and experimental data. Furthermore, an improved new design was suggested to further increase the heat transfer performance and create uniformity of temperature distribution.

**Keywords:** Fluid flow, Heat Transfer, Microchannel, Heat Sink, Computational Fluid Dynamics

## 1. Introduction

Miniaturization of electronic devices has led to advances in various engineering fields, including space technology, defense systems, aerospace applications, manufacturing technology, industrial processes and consumer electronics [1]. Heat dissipation in the electronic components, however, is being a critical issue due to the faster increase in the components' heat flux and increasing demand for the miniature in features' size. The heat flux of the electronic chips may exceed  $400 \text{ W/cm}^2$  in order to meet the demand for high performance electronic components. Since overheating of the electronic components degrades the components' performance, reliability and even cause failure of the components, high performance cooling techniques are required to keep device temperatures low for acceptable performance and reliability [2-5].

The microchannel heat sink (MCHS) is a concept well suited for many electronic applications because of its ability to remove a large amount of heat from a small area [6]. Over the past two decades, a large number of experimental, theoretical and numerical simulation on the fluid flow and heat transfer in microchannel have been reported to provide useful data to comprehensively understand the physical mechanisms under various operating conditions and to optimize their design. A review of the fundamental investigations relevant to the single-phase convective heat transfer in microchannels can be traced back to Morini [7]. It is recognized that extensive research works has been devoted to flow and heat transfer performance in microchannel in most recent years, thus, this review can not include every paper, some selection is necessary.

Soleimanikutanaei et al. performed a three-dimensional numerical study to investigate the heat transfer performance through the use of transverse microchannles in a heat sink [8]. Their results indicated that the temperature distribution and the location of hotspots were dependent on the number and size of transverse microchannels at different Reynolds numbers. Li et al. numerically

50 studied the flow structure and heat transfer performance of water-cooled microchannel heat sink  
51 with dimple and pin-fin [9]. It was found that their proposed designs could achieve heat transfer  
52 augmentation with potential energy saving and low resistance. Yin et al. experimentally  
53 investigated the pressure drop and heat transfer performance of the deionized water flow boiling in  
54 open microchannels [10]. Their results showed that, in stratified flow regimes, a better heat  
55 dissipation capability was achieved when the size of the open microchannel is small but with great  
56 number of channels. Prajapati numerically studied the fluid flow and heat transfer behavior in seven  
57 different rectangular parallel microchannel heat sinks with different fin height for the Reynolds  
58 numbers varied from 100 to 400 and heat flux ranged from 100 to 500 kW/m<sup>2</sup> [11]. Their predicted  
59 results showed that the heat sink with fin height of 0.8 mm exhibited maximum heat transfer.  
60 Kumar carried out a combined three-dimensional numerical simulation and experimental work to  
61 investigate the fluid flow and heat transfer in trapezoidal microchannel heat sink for the Reynolds  
62 number ranged from 96 to 720 [12]. They concluded that trapezoidal shaped channels could have  
63 prominent advantages over rectangular microchannels with 12% enhancement in heat transfer. Liu  
64 et al. proposed two novel annular microchannel heat sink designs and analyzed the flow distribution  
65 and substrate temperature uniformity [13]. Both experimental and numerical results showed that  
66 temperature uniformity of the interleaved arrangement is better than that of the sequential  
67 arrangement. Chai et al. developed a three-dimensional conjugate heat transfer model to investigate  
68 the local laminar fluid flow and heat transfer characteristics in microchannel heat sinks with  
69 tandem triangular ribs for the Reynolds number of 443 [14]. Their numerical results showed clearly  
70 that the triangular ribs could significantly reduce the temperature rise of the heat sink base and  
71 could also prevent the drop of the local heat transfer coefficient efficiently along the flow direction.  
72 As a series of study, the same researchers conducted a sensitivity study to analyze the average  
73 laminar fluid flow and heat transfer characteristics [15]. They proposed new fluid flow and heat  
74 transfer correlations for the microchannel heat sinks with triangular ribs on sidewalls and good  
75 agreements was achieved compared with computational results within their current operating  
76 conditions. Dey et al. performed a three-dimensional numerical simulation and experimental study  
77 on the fluid flow and heat transfer characteristics of novel fish scale bioinspired structures at the  
78 bottom surface of microchannel using deionized water as the working fluid [16]. Their results found  
79 that the bioinspired surface could enhance the convective heat transfer compared to the plain  
80 microchannel, whereas the pressure drop was found less. Ma et al. experimentally studied the flow  
81 and heat transfer characteristics in the silicon microchannel heat sinks with periodic jetting or  
82 throttling structures using deionized water as the working fluid with flow rates of 28-95 ml/min [17].  
83 It was concluded that the heat transfer of throttling microchannel heat sink is obviously enhanced  
84 although the pressure is large. Bayrak et al. performed a comparative analysis to investigate the  
85 thermal-hydraulic performances of several different microchannel heat sink designs for cooling  
86 channels in a lithium-ion battery [18]. It was observed that local modifications in channels can  
87 ensure suitable fluid mixing between core flow and near wall regions which can enhance the heat  
88 transfer performance considerably compared to the microchannel design with no cavity and rib.  
89 Wang et al. conducted a combined experimental and numerical study on the flow and heat transfer  
90 characteristics of microchannel heat sink with bidirectional ribs [19]. It revealed that the higher  
91 relative rib height of vertical rib and relative rib width of spanwise rib can enhance the heat transfer  
92 but induce the pressure drop. Yang and Cao carried out a three-dimensional numerical study to  
93 investigate the flow and heat transfer characteristics of a novel hybrid microchannel heat sink with  
94 manifold arrangement and secondary oblique channels [20]. They defined a region named design  
95 optimization area where both the pressure drop and the total thermal resistance can be reduced due  
96 to secondary channels. Shi et al. employed a multi-objective evolutionary algorithm to investigate  
97 the flow and heat transfer characteristics of a microchannel heat sink with secondary flow channel  
98 for optimal design [21]. It was stated that the performance of the microchannel heat sink with  
99 secondary flow channel can be significantly improved by optimization of the structure parameters.

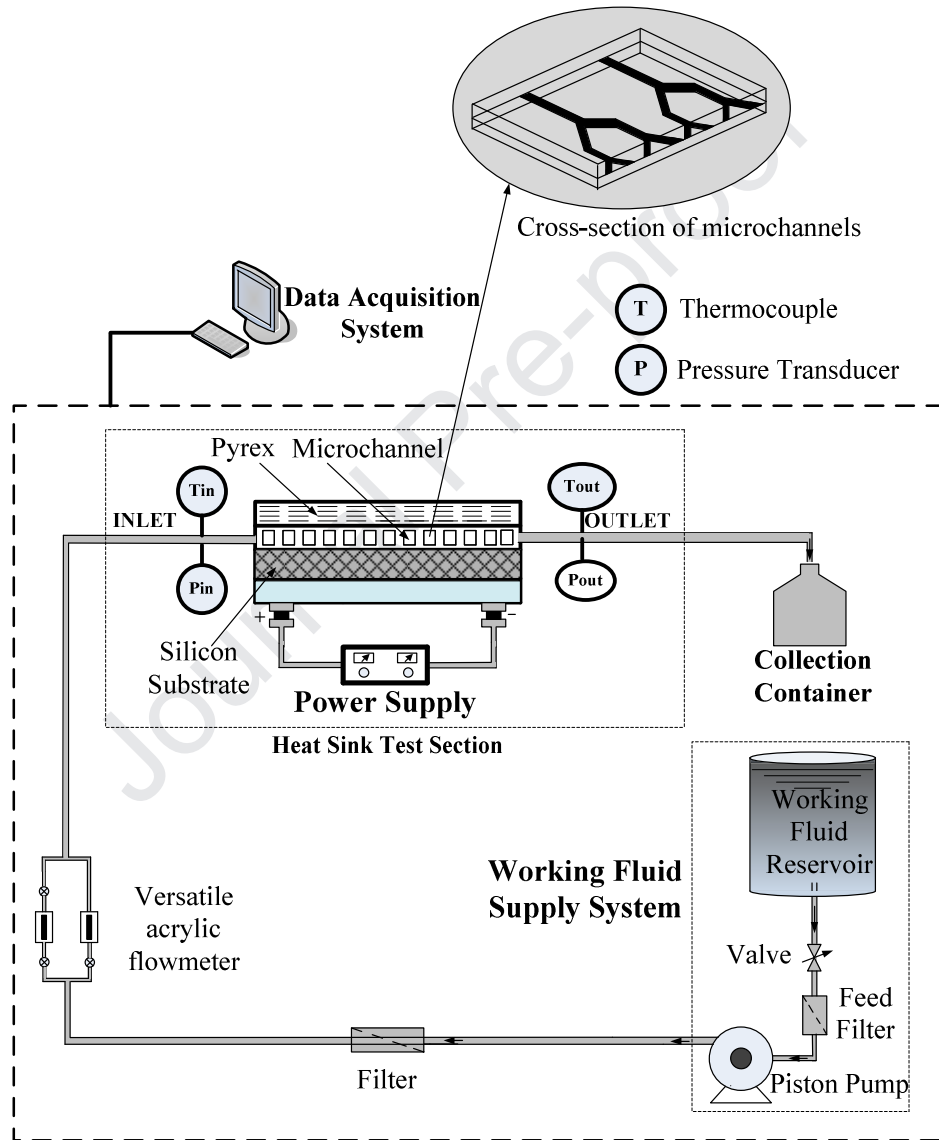
100 Although many significant results in the flow and heat transfer characteristics of microchannel  
101 have already been obtained, the comprehension of the flow and heat transfer mechanism of Y-

102 fractal microchannel is still quite limited. The present work aims to investigate the flow and heat  
 103 transfer in a Y-fractal microchannel both experimentally and numerically. In order to elucidate the  
 104 pertinent physical phenomena involved in the study, further calculation based on the validated CFD  
 105 model on a new type of microchannel is numerically demonstrated.

## 106 2. Experimental and computational details

### 107 2.1. Experimental apparatus and method

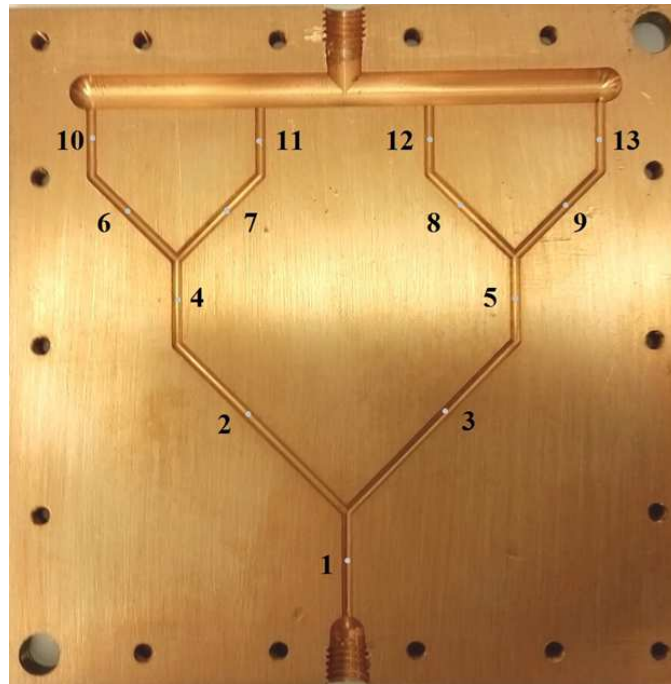
108 In the current study, a new experimental test rig was constructed. Figure 1 presented the  
 109 schematic diagram of the overall layout of the experimental system, which is mainly composed of  
 110 the water cooling circulation subsystem, heating system, test section and data acquisition system.  
 111



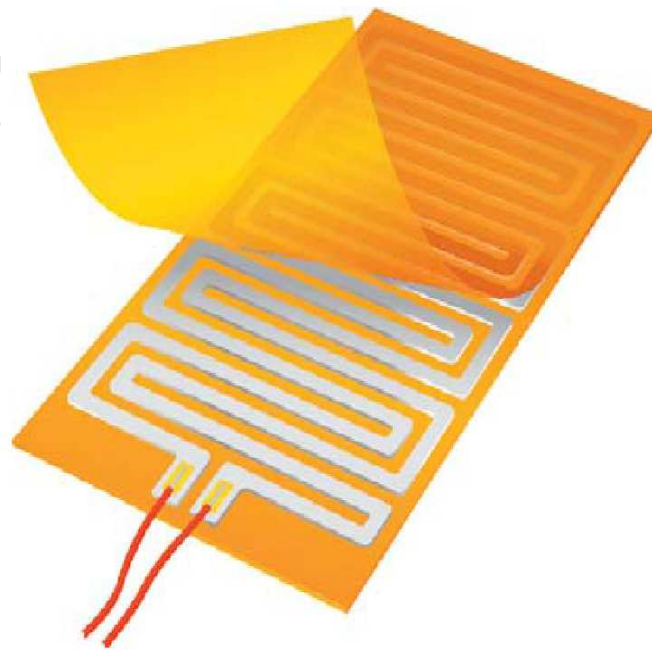
112  
 113  
 114 Figure 1. The schematic diagram of the experimental system.  
 115

116 The main components of the water cooling circulation subsystem include a pump, mass flow  
 117 meter, thermostatic water tank. In the water cooling circulation system, the water inlet temperature  
 118 is controlled by a recirculating digital water bath (SWB23-2, USA) with an accuracy of  $\pm 0.2$  °C.  
 119 Water circulation in the loop is maintained by a peristaltic pump (Watson Marlow Model). A  
 120 versatile acrylic flowmeter (Cole Palmer) is chosen to provide accurate flow measurement with an  
 121 accuracy of  $\pm 5\%$  FS.

122 Figure 2 shows a picture of the designed microchannel that is manufactured using the computer  
123 numerical control (CNC) machine. The copper is selected as the test section material with  
124 dimension of 10 cm (W) x 10 cm (H) x 6 mm (D), as shown in Figure 2(a). And the diameter of the  
125 microchannel is 1.5 mm. The polyimide film heating element of dimensions 80 mm x 80 mm and  
126 1.52 mm thickness (see Figure 2(b)) that attached to the bottom of the microchannel is connected to  
127 a DC power supply (EA-PS 2042-20B) with maximum power output of 300 W to deliver the  
128 heating power to the copper. A Rosemount 3051S pressure transmitter (Emerson) with an accuracy  
129 of  $\pm 0.025\%$  FS is chosen to measure the pressure drop between the inlet and outlet of the test  
130 section. In the current study, water is selected as the working fluid.



(a)



(b)

Figure 2. Microchannel test section (a) and heating element (b).



174 The test section is instrumented with thirteen type K thermocouples which are spot welded  
 175 directly to the outer surface of the copper wall during each test run. The thermocouples are located  
 176 at number 1, 2, ...13, as illustrated in Figure 2(a). Each thermocouple with an accuracy of  $\pm 0.5$  °C  
 177 is calibrated prior to testing in order to check and correct for induced temperature bias error that  
 178 caused by the voltage across the test section. In the experiments, the whole test section was covered  
 179 by a heat insulation material (glass wool) with thermal conductivity of less than 0.012 W/(m K) to  
 180 reduce heat loss.

## 181 2.2. Data acquisition

182 The main components of the data acquisition system include temperature sensors, a data  
 183 acquisition unit (Agilent 34970A) and a computer. The experimental data will be recorded every  
 184 second by using Agilent 34970A and collected in the computer.

## 185 2.3. Experimental procedure

186 In the current study, three typical runs are conducted during the experiment. In the first  
 187 experiment, keeping the heat flux and water inlet temperature constant, the inlet velocity is changed  
 188 from 0.6 to 1.0 L/min at an interval of 0.1 L/min. The second experiment is carried out while  
 189 keeping the inlet flow rate and inlet temperature constant, but increasing the heat flux from  $1.0 \times 10^4$   
 190 to  $2.5 \times 10^4$  W/m<sup>2</sup>. In the third set of experiments, both flow rate and heat flux are kept constant but  
 191 the inlet flow temperature is changed. The experimental conditions are summarized in Table 1.  
 192

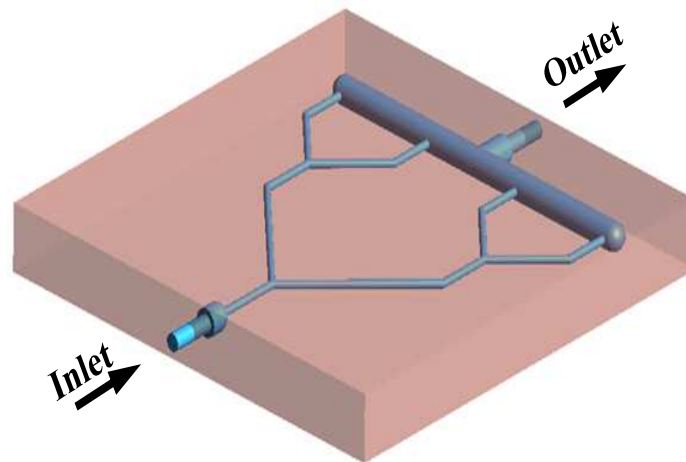
193 Table 1. Experimental conditions

Parameter	Unit	Range
Flow rate	L/min	0.6 – 1.0
Heat flux	W/m <sup>2</sup>	$1 \times 10^4$ – $2.5 \times 10^4$
Inlet temperature	K	323.15 – 348.15

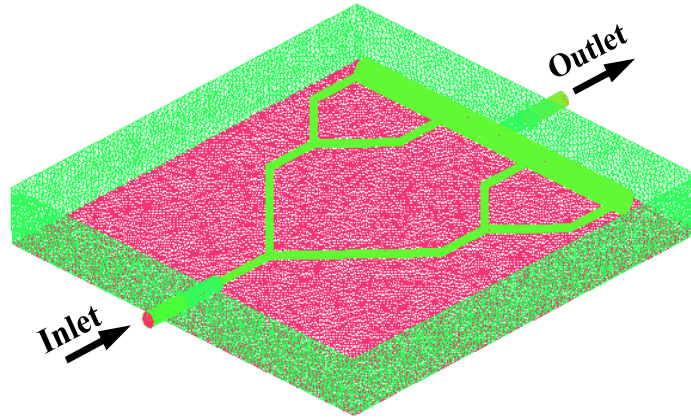
194

## 195 2.4. Computational model

196 For the purpose of comparison and further calculation, the CFD study chooses the same  
 197 geometry of the experimental work outlined above as the computational domain, as shown in Figure  
 198 3(a) and Figure 3(b).  
 199



(a)



(b)

Figure 3: (a) Geometry and (b) computational domain.

In the current work, a grid independence study is performed by using different grids and a compromise between computation accuracy and computing capability led to the use of 1.3 million cells. In the current study, a standard  $k-\mathcal{E}$  turbulence model is employed. To comply with the experiments, the boundary conditions are set as following: 293 K for the water temperature at inlet of the test section, the flow rate is set to be 1.0 L/min, the heat flux at the bottom surface of the test section is  $2.5 \times 10^4 \text{ W/m}^2$ , and the other walls are set to be thermally insulated. The outlet is set constant pressure at 1 atm. The simulation is performed using commercial CFD Fluent solver.

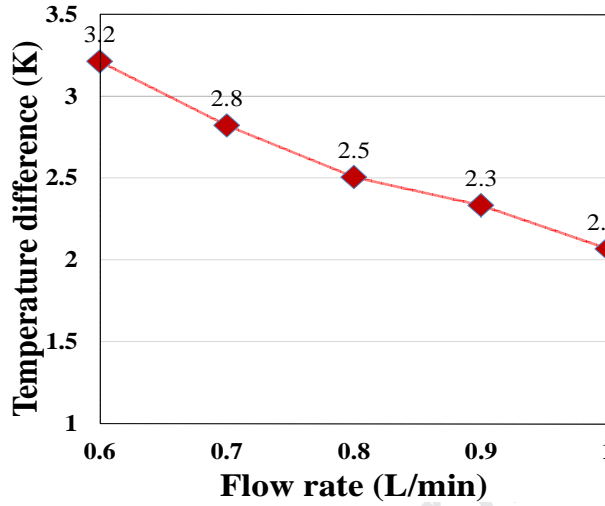
### 3. Results and discussion

In the following sections, the effects of several typical control parameters, such as flow rate and heat flux, on the temperature difference across the test section are discussed experimentally. Afterwards, the developed numerical model will be firstly evaluated through the comparison of the temperature drops between the numerical results and the experimental data. Then the flow characteristics and the temperature distribution will be examined as a case study. Finally, a CFD simulation on a new designed MCHS will be discussed based on the developed CFD model.

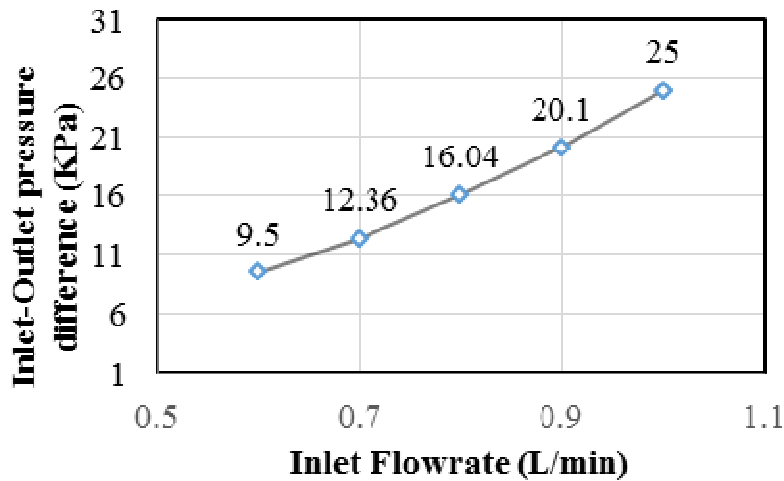
#### 3.1. Sensitivity analysis

Figure 4(a) shows the effect of the variation of the flow rate on the temperature difference under steady state operating conditions. In this study, experiments are conducted for five different flow rates: 0.6, 0.7, 0.8, 0.9 and 1.0 L/min, and the water temperature and heat flux are kept constant, which are 293 K and  $1.0 \times 10^4 \text{ W/m}^2$ , respectively. Under the operating conditions studied, as is expected, the effect of flow rate is apparent. It can be seen clearly from Figure 4(a) that the temperature difference decreases with the increase of the flow rate of the working fluid. It can be noted that the temperature difference is reduced from 3.2 to 2.1 °C when the flow rate increased from 0.6 to 1.0 L/min. Figure 4(b) presents the pressure drop across the test section at five different flow rates, i.e. 0.6, 0.7, 0.8, 0.9 and 1.0 L/min. It is observed in Figure 4(b) that the pressure drop increases monotonously with the increase of flow rate. It should be noted that the higher flow rate have a significant effect on the pressure drop. This can be demonstrated that the pressure drop increased from 20.1 KPa at flow rate of 0.9 L/min to 15 KPa at 1.0 L/min, whereas the pressure drop increased from 9.5 KPa at 0.6 L/min to 12.36 KPa at 0.7 L/min. Figure 4(c) demonstrates the variation of the temperature difference for heat flux applied from  $1.0 \times 10^4$  to  $2.5 \times 10^4 \text{ W/m}^2$  in an increment of  $5 \times 10^3 \text{ W/m}^2$  at a fixed flow rate of 1.0 L/min. From Figure 4(c), it can be seen clearly that the linear nature of relation between change in temperature and heat flux. As the heat flux applied to the heat sink increases, the flowing water through it is able to take more heat away by

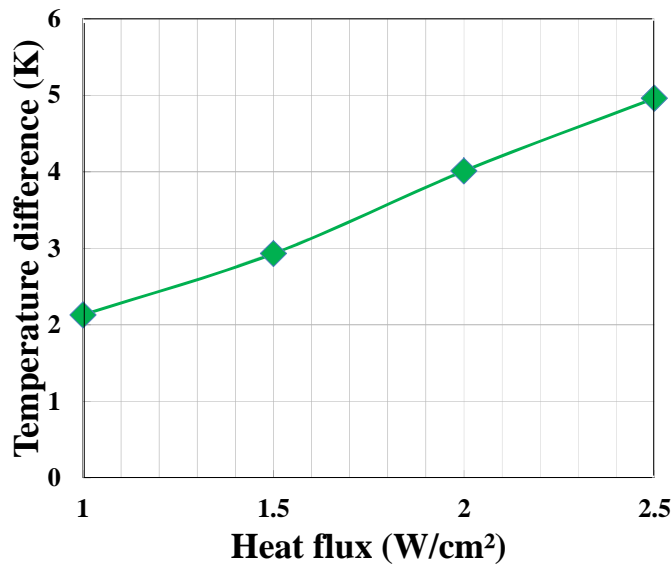
237 convection. Note also that the temperature difference is reduced from 2.1 to 5 °C when the heat flux  
 238 is increased from 1 to 2.5 W/m<sup>2</sup>. The effects of water inlet temperature on the temperature  
 239 difference across the test section are depicted in Figure 4(d). It can be observed from Figure 4(d)  
 240 that as the temperature of coolant at inlet increases, the rate at which heat is carried out of the  
 241 system decreases. This indicates that too much higher inlet temperature does not have a significant  
 242 effect on the cooling.



243 (a) Effect of flow rate on temperature difference.  
 244

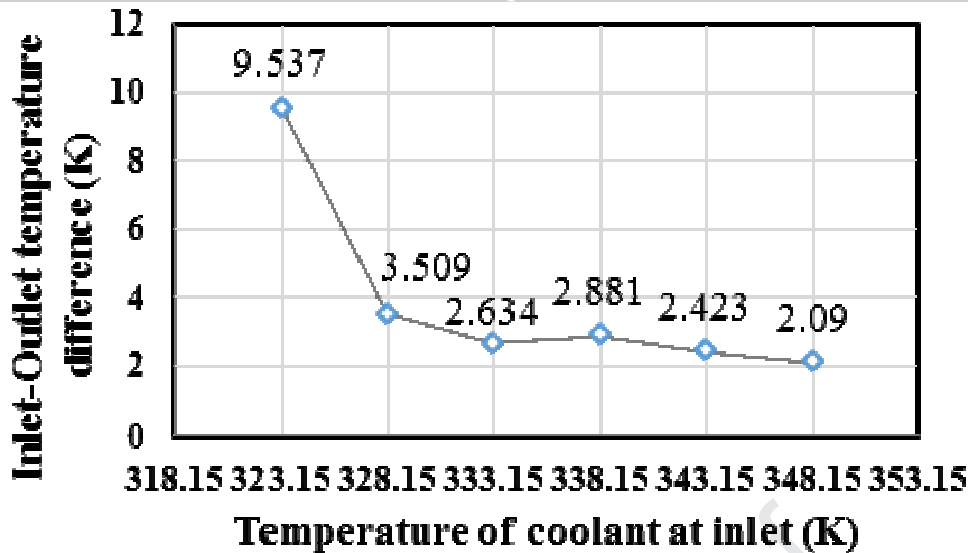


245 (b) Pressure drop vs flow rate.  
 246



247 (c) Effect of heat flux on temperature difference.  
 248





(d) Effect of water inlet temperature on temperature difference.

Figure 4: Sensitivity analysis.

249  
250  
251  
252  
253  
254  
255  
256  
257  
258

### 3.2. Model validation

Prior to conducting the aimed computations, in the current study, it is necessary to validate the computational model. Figure 5 shows the comparison of the temperature difference across the test section between the numerical results and experimental data at five different flow rates of 0.6, 0.7, 0.8, 0.9 and 1.0 L/min while the water inlet temperature and heat flux are fixed.

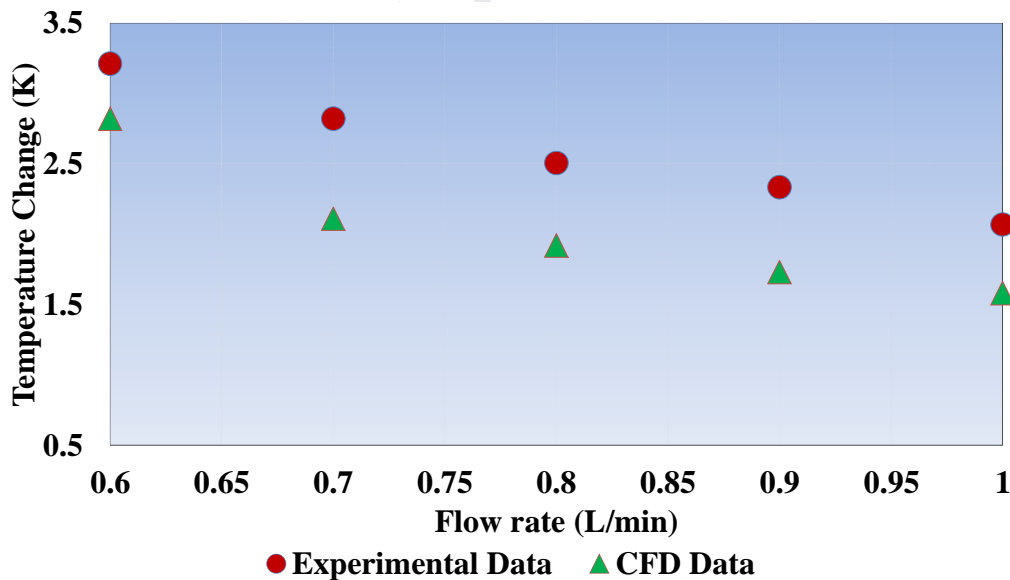


Figure 5: Comparison of computed and measured temperature difference between the inlet and outlet of the test section.

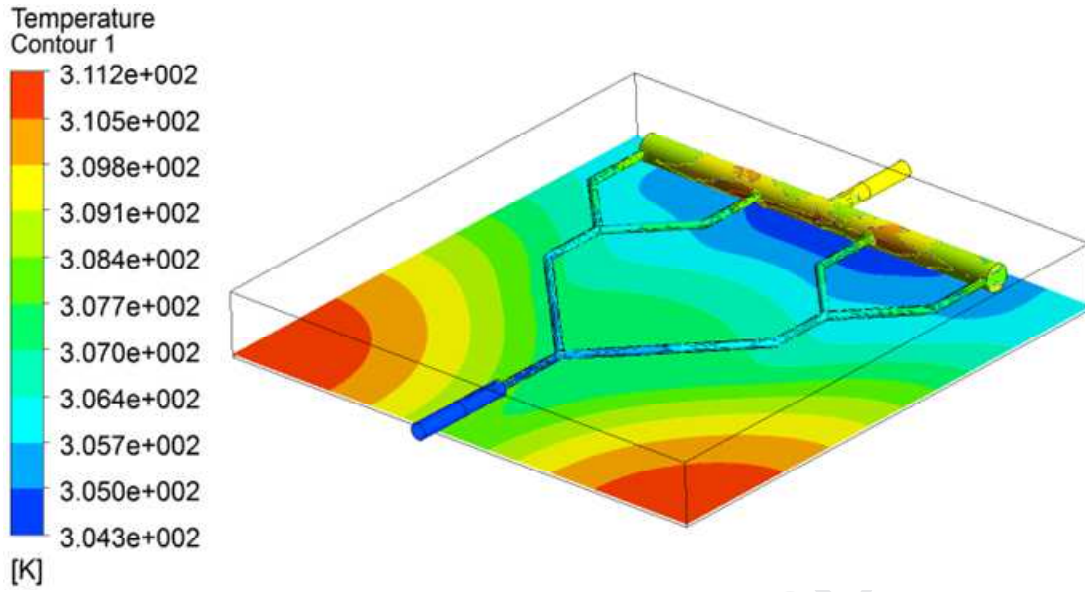
259  
260  
261  
262  
263  
264  
265  
266  
267  
268  
269  
270

From Figure 5, it can be seen clearly that in general there is a good agreement between the currently predicted results and the experimental data with an accuracy of less than 1%.

### 3.3. Flow and heat transfer analysis

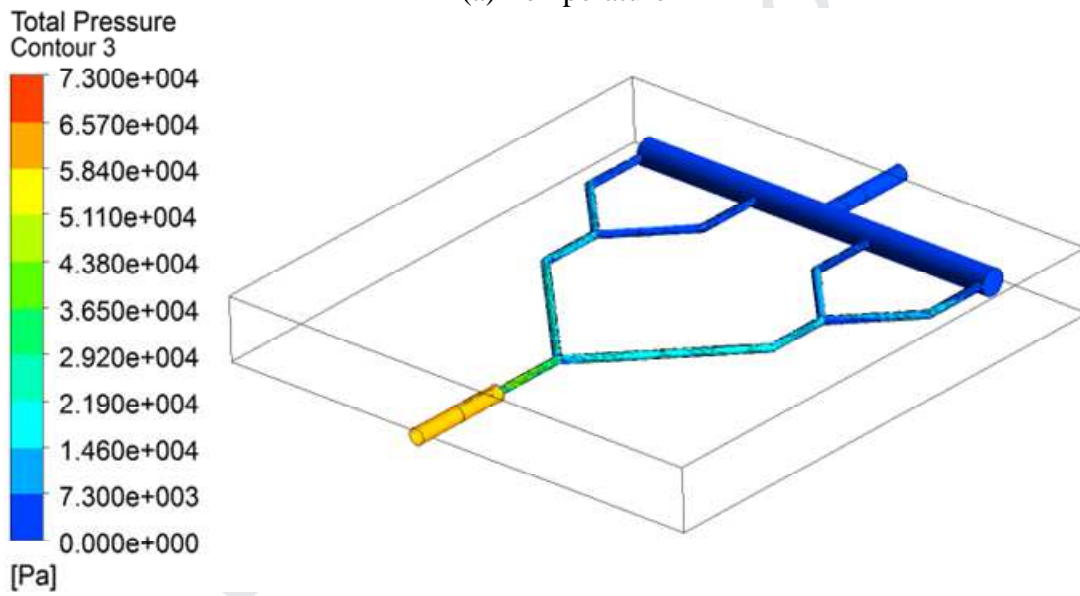
It is believed that the fluid flow alters the temperature on the copper plate when a constant heat flux is applied at the bottom. Based on the CFD simulation results, Figure 6 exhibits the profiles of contour temperature, pressure and velocity of the microchannel at steady state when a constant water inlet temperature (293 K), flow rate (1.0 L/min) and heat flux ( $2.5 \times 10^4 \text{ W/m}^2$ ) is applied.

271



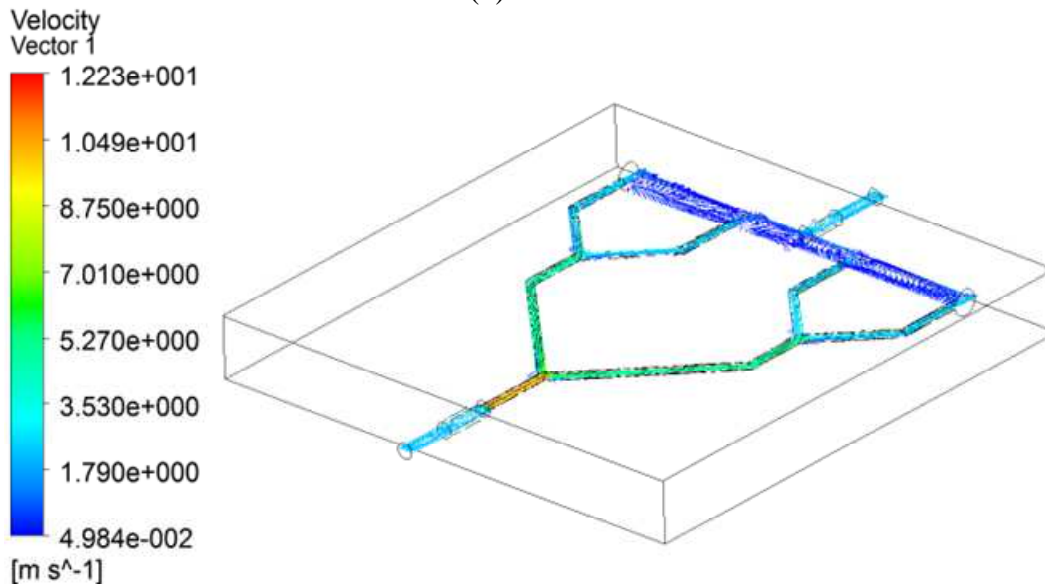
272  
273

(a) Temperature



274  
275

(b) Pressure



276  
277  
278

(c) Velocity

Figure 6: (a) Temperature, (b) pressure and (c) velocity profile of the microchannel.

279 As shown in Figure 6(a), the plate's surface temperature is down close to the channels as the  
280 water is dissipating the heat away but some hot spots as observed as the red regions in the Figure.  
281 The temperature in plate near the outlet is very low since the presence of comparatively more  
282 channels in the region. It is easy to understand from Figure 6(b) that a high pressure is achieved at  
283 the inlet of the test section. As water goes further, the pressure decreases till the atmospheric  
284 pressure is achieved. Figure 6(c) indicates that the contour of the velocity inside the microchannel.  
285 It is clearly seen that the velocity is dominated by the shape of the microchannel.  
286

#### 287 4. Conclusions

288 For the purpose of elucidating the detailed processes pertinent to microchannel cooling  
289 technology, in the present study, a Y-fractal microchannel based heat sink was designed,  
290 manufactured and tested to investigate the effects of three different control parameters, i.e. fluid  
291 flow rate, heat flux and inlet temperature, on the flow and heat transfer characteristics. The  
292 comparison between the calculated results and experimental data was carried out. Results show that  
293 close agreement is achieved between the computed results and experimental data. The results of this  
294 study could substantially contribute to the state of knowledge regarding flow and heat transfer in  
295 microchannel. The research provides an enhanced understanding of thermal performance and the  
296 potential for improvements. Future work will investigate the flow and heat transfer characteristics  
297 using nanofluid as the working fluid. Machine learning would be a promising approach in  
298 prediction for microchannel if big data are available.  
299

#### 300 Acknowledgments

301 The authors would like to thank the financial support from State Grid Coporation of China  
302 Research Program "Preliminary Study of Frequency Modulation Technology for Power Grid Based  
303 on Compressed Air Energy Storage" (SGZJ0000KXJS1800283). Project No: GEIRI-DL-71-18-002.

#### 304 References

- 305 [1] H. Ganapathy, A. Shooshtari, K. Choo, S. Dessiatoun, M. Alshehhi, M. Ohadi, Volume of fluid-  
306 based numerical modelling of condensation heat transfer and fluid flow characteristics in  
307 microchannels, *International Journal of Heat and Mass Transfer*, 65:72-72, 2013.
- 308 [2] M. Kalteh, A. Abbassi, M. Saffar-Avval, A. Frijns, A. Darhuber, J. Harting, Experimental and  
309 numerical investigation of nanofluid forced convection inside a wide microchannel heat sink,  
310 *Applied Thermal Engineering*, 36:260-268, 2012.
- 311 [3] B. Fani, A. Abbassi, M. Kalteh, Effect of nanoparticles size on thermal performance of  
312 nanofluid in a trapezoidal microchannel-heat-sink, *International Communications in Heat and Mass*  
313 *Transfer*, 45:155-161, 2013.
- 314 [4] P. Selvakumar, S. Suresh, S. Salyan, Investigations of effect of radial flow impeller type swirl  
315 generator fitted in an electronic heat sink and Al<sub>2</sub>O<sub>3</sub>/water nanofluid on heat transfer enhancement,  
316 *Chemical Engineering and Processing: Process Intensification*, 72:103-112, 2013.
- 317 [5] J.F. Tullius, Y. Bayazitoglu, Effect of Al<sub>2</sub>O<sub>3</sub>/H<sub>2</sub>O nanofluid on MWNT circular fin structures  
318 in a minichannel, *International Journal of Heat and Mass Transfer*, 60:523-530, 2013.
- 319 [6] M. Rahimi, E. Karimi, M. Asadi, P. Valeh-e-Sheyda, Heat transfer augmentation in a hybrid  
320 microchannel solar cell, *International Communications in Heat and Mass Transfer*, 43:131-137,  
321 2013.
- 322 [7] G. L. Morini, Single-phase convective heat transfer in microchannels: a review of experimental  
323 results, *International Journal of Thermal Sciences*, 43:631-651, 2004.
- 324 [8] S. Soleimanikutanaei, E. Ghasemisahebi, C. Lin, Numerical study of heat transfer enhancement  
325 using transverse microchannels in a heat sink, *International Journal of Thermal Sciences*, 125:89-  
326 100, 2018.

- 327 [9] P. Li, Y. Luo, D. Zhang, Y. Xie, Flow and heat transfer characteristics and optimization study  
328 on the water-cooled microchannel heat sinks with dimple and pin-fin, *International Journal of Heat*  
329 *and Mass Transfer*, 119:152-162, 2018.
- 330 [10] L. Yin, P. Jiang, R. Xu, H. Hu, L. Jia, Heat Transfer and pressure drop characteristics of water  
331 flow boiling in open microchannels, *International Journal of Heat and Mass Transfer*, 137:204-215,  
332 2019.
- 333 [11] Y.K. Prajapati, Influence of fin height on heat transfer and fluid flow characteristics of  
334 rectangular microchannel heat sink, *International Journal of Heat and Mass Transfer*, 137:1041-  
335 1052, 2019.
- 336 [12] P. Kumar, Numerical investigation of fluid flow and heat transfer in trapezoidal microchannel  
337 with groove structure, *International Journal of Heat and Mass Transfer*, 136:33-43, 2019.
- 338 [13] H. Liu, D. Qi, X., Shao, W. Wang, An experimental and numerical investigation of heat  
339 transfer enhancement in annular microchannel heat sinks, *International Journal of Thermal*  
340 *Sciences*, 142:106-120, 2019.
- 341 [14] L. Chai, L. Wang, X., Bai, Thermohydraulic performance of microchannel heat sinks with  
342 triangular ribs on sidewalls – Part 1: Local fluid flow and heat transfer characteristics, *International*  
343 *Journal of Thermal Sciences*, 127:1124-1137, 2019.
- 344 [15] L. Chai, L. Wang, X., Bai, Thermohydraulic performance of microchannel heat sinks with  
345 triangular ribs on sidewalls – Part 2: Average fluid flow and heat transfer characteristics,  
346 *International Journal of Thermal Sciences*, 128:634-648, 2019.
- 347 [16] P. Dey, G. H, S.K. Saha, Experimental and numerical investigations of fluid flow and heat  
348 transfer in a bioinspired surface enriched microchannel, *International Journal of Thermal Sciences*,  
349 135:44-60, 2019.
- 350 [17] D. Ma, G. Xia, W. Wang, Y. Jia, Y. Yang, Study on thermal performance of microchannel heat  
351 sinks with periodic jetting and throttling structures in sidewalls, *Applied Thermal Engineering*,  
352 158:113764, 2019.
- 353 [18] E. bayrak, A.B. Olcay, M.F. Serincan, Numerical investigation of the effects of geometric  
354 structure of microchannel heat sink on flow characteristics and heat transfer performance,  
355 *International Journal of Thermal Sciences*, 135:589-600, 2019.
- 356 [19] G. Wang, N. Qian, G. Ding, Heat transfer enhancement in microchannel heat sink with  
357 bidirectional rib, *International Journal of Heat and Mass Transfer*, 136:597-609, 2019.
- 358 [20] M. Yang, B. Cao, Numerical study on flow and heat transfer of a hybrid microchannel cooling  
359 scheme using manifold arrangement and secondary channels, *Applied Thermal Engineering*, (in  
360 press)
- 361 [21] X. Shi, S. Li, Y. Mu, B. Yin, Geometry parameters optimization for a microchannel heat sink  
362 with secondary flow channel, *International Communications in Heat and Mass Transfer*, 104:89-  
363 100, 2019.

## **Conflict of Interest Statement**

We declare that we have no financial and personal relationships with other people or organizations that can inappropriately influence our work, there is no professional or other personal interest of any nature or kind in any product, service and/or company that could be construed as influencing the position presented in, or the review of, the manuscript entitled “Flow Characteristics and Heat Transfer Performance in a Y-Fractal Mini/Microchannel Heat Sink”.

Yours Sincerely,

Hongwei Wu

School of Engineering and Computer Science  
University of Hertfordshire  
Hatfield, AL10 9AB, United Kingdom